Available online at www.sciencedirect.com
ScienceDirect
International Journal of Plasticity xxx (2007) xxx–xxx
INTERNATIONAL JOURNAL OF Plasticity
www.elsevier.com/locate/ijplas

On XFEM applications to dislocations and interfaces

Ted Belytschko *,[1], Robert Gracie

Department of Mechanical Engineering, Northwestern University, 2145 Sheridan Road, Evanston, IL 60208-3111, USA

Received 15 October 2006; received in final revised form 10 February 2007

Dedicated to Dusan Krajcinovic, whose work in damage mechanics and plasticity was illuminating and invaluable to the mechanics community.

Abstract

A method for modelling dislocations in systems with arbitrary materials interfaces is described. The method is based on the extended finite element method (XFEM) where dislocations are modelled in the manner of the Volterra dislocation model. A method for calculating the Peach–Koehler force by *J*-integrals in this framework is studied. The method is compared to closed form solutions for interface problems and excellent accuracy is obtained. The convergence and accuracy of the method is studied in two problems where analytical solutions are available: an edge dislocation interacting with a free-surface and an edge dislocation interacting with a bimaterial interface. The applicability of the method to more complicated problems is illustrated by the modelling of slip misorientation of an edge dislocation with a glide plane intersecting a material interface and dislocations in a multi-material domain with non-parallel interfaces.

Keywords: Dislocations; Interfaces; Extended finite element method; Peach–Koehler force

1. Introduction

Computational Dislocation Dynamics (DD) is increasingly being applied to the resolution of important questions in nonlinear bulk material behaviour and plasticity,

* Corresponding author.
E-mail address: tedbelytschko@northwestern.edu (T. Belytschko).
[1] Walter P. Murphy and McCormick Professor of Mechanical Engineering.

0749-6419/$ - see front matter © 2007 Published by Elsevier Ltd.
doi:10.1016/j.ijplas.2007.03.003

Please cite this article in press as: Belytschko, T., Gracie, R., On XFEM applications to dislocations..., Int. J. Plasticity (2007), doi:10.1016/j.ijplas.2007.03.003

e.g. Amodeo and Ghoniem (1990), Canova et al. (1993), Van der Giessen and Needleman (1995), Zbib et al. (1998), Ghoniem et al. (2000), Shehadeh et al. (2005). Of interest more recently are applications involving micro/nano scale systems. For example, Polonsky and Keer (1996) used DD to model plasticity due to contact in micro-scale systems; Nicola et al. (2005) have computationally reproduced size effects in thin films; Balint et al. (2006) have studied size effects in crystals and polycrystals; Espinosa et al. (2006) have shown size effects in freestanding FCC films and partially calibrated them by experiments. Usually, these computational methods are based on superposition of infinite domain analytical solutions. For micro/nano scale systems, the effects of boundaries, material interfaces and material anisotropy are important; however, the extension of existing methods to these problems is difficult, since the existence of Green's function for specific geometries is limited, see Ghoniem and Han (2005).

Alternative methods are the phase field method (PFM) of Wang et al. (2001) and the level set based method of Xiang et al. (2003). The PFM, like the proposed method, directly models the displacement field but represents the discontinuities of the dislocations by regularizations. Both methods have been applied with fast Fourier transforms, though in principle they can be applied with standard finite elements. Another method which directly approximates the displacement field due to the dislocations is that of Lemarchand et al. (2001), where the effect of the dislocations in the continuum is introduced through a plastic strain.

In DD a sequence of equilibrium solutions must be obtained with evolving dislocations; at each step the total stress of the domain is determined for a given distribution, number and geometry of the dislocations. The geometry, number and location of the dislocations for the next step of the simulation are determined using a phenomenological equation of motion for each dislocation, where the Peach–Koehler force is the driving force, and a set of rules, which govern among other things, dislocation nucleation and annihilation.

The DD codes based on superposition determine the total stress of the domain by the sum of the analytical solutions of dislocations in an infinite domain plus an image stress field. In three-dimensional methods, these solutions usually take the form of Green's functions. Methods based on superposition are difficult to extend to important problems such as anisotropic materials and material interfaces. With the exception of a few geometries, such as the recently developed Green's functions of Ghoniem and Han (2005) and Han and Ghoniem (2005) for parallel anisotropic materials, Green's functions cannot readily be obtained for anisotropic materials with arbitrary material interfaces. Therefore, methods based on Green's functions for these applications will be difficult to develop.

We describe some studies with a method we have recently developed (Gracie et al., 2007), that is easily able to treat anisotropic materials, interfaces and grain boundaries. The methodology is based on the extended finite element method (Belytschko and Black, 1999; Moës et al., 1999; Belytschko et al., 2001), in which an arbitrary discontinuity is added to a finite element solution independent of the mesh, i.e. the discontinuity does not need to conform to the mesh in any way. This enables the method to model a dislocation as described originally by Volterra (1907): an interior discontinuity that results from cutting a solid, displacing the two opposing surfaces and then regluing the solid along the cut. The stresses that are computed by an XFEM calculation correspond to those that would result from this process. The work of Ventura et al. (2005) which proposed a dislocation model based on a similar finite element method, the Partition of Unity Method, was particularly influential to the current work.

Please cite this article in press as: Belytschko, T., Gracie, R., On XFEM applications to dislocations..., Int. J. Plasticity (2007), doi:10.1016/j.ijplas.2007.03.003

To account for finite domain boundary conditions, superposition methods require the computation of an image field. In Fivel et al. (1996), the image stress is determined by a method based on the Boussinesq problem, while in the method of Van der Giessen and Needleman (1995) it is computed by the finite element method. In contrast, the method presented here uses a finite element method (FEM) to compute the total stress field.

Here we examine the suitability of the *J*-Integral for computing the Peach–Koehler force. Since the method presented here does not use superposition, the self-stress of a dislocation cannot simply be subtracted out of the total stress. So the Peach–Koehler formula, (Peach and Koehler, 1950), cannot be applied. We show that the *J*-Integral is effective for computing the Peach–Koehler force and discuss its relative advantages and disadvantages.

From the examples considered here, the extension of the method to anisotropic materials and grain boundaries will become apparent. The ability of the method to easily model problems involving interfaces is one of its principal advantages. Here, we will illustrate the effectiveness of the method for problems involving interfaces, albeit in some rather simple problems.

In the following section, we summarize the methodology and the discrete equations of the proposed method. In Section 3 we discuss the computation of the Peach–Koehler force by the *J*-integral. In Section 4 we apply the proposed method to problems involving interfaces and in Section 5 we present the conclusions.

2. Methodology

We first briefly review the method for modelling dislocations. Consider the domain Ω bounded by Γ with tractions $\boldsymbol{t}$ defined on boundary Γ_t, displacements $\bar{\mathbf{u}}$ defined on boundary Γ_u and with internal surfaces of discontinuity α, $\alpha = 1$ to n_D, that model the n_D dislocations Γ_d^α. We define $\Gamma_d = \bigcup_\alpha \Gamma_d^\alpha$. While the method is applicable to any type of dislocation, we restrict this paper to edge dislocations.

The geometry of dislocation α is described by an affine function of the coordinates, $f^\alpha(\mathbf{x}) = 0$, where

$$f^\alpha(\mathbf{x}) = \alpha_0 + \alpha_j x_j \tag{1}$$

and repeated indices denote summations. The core is described by the intersection of the glide plane, $f^\alpha(\mathbf{x}) = 0$, and a distance function (or level set function) $g^\alpha(\mathbf{x}) = 0$ where $g^\alpha(\mathbf{x}) > 0$ on the active portion of the slip plane.

Let $\mathscr{S}$ be the set of all nodes, $\mathscr{E}^\alpha$ be the set of all elements cut by discontinuity α and $\mathscr{S}^\alpha$ be the set of enriched nodes for dislocation α; the latter is the set of all nodes of elements in $\mathscr{E}^\alpha$. A virtual element is superimposed on the element containing the dislocation core, as shown in Fig. 1, so that the corner node is coincident with the center of the core. The core node of dislocation α is denoted by C^α and $C^\alpha \in \mathscr{S}^\alpha$. The displacement approximation for the continuum containing n_D dislocations with Burger's vectors $\boldsymbol{b}^\alpha$ has the form

$$\mathbf{u}(\mathbf{x},t) = \sum_{I\in\mathscr{S}} N(\mathbf{x})_I \mathbf{u}_I(t) + \sum_{\alpha=1}^{n_D} \mathbf{b}^\alpha \sum_{J\in\mathscr{S}^\alpha} \widetilde{N}_J(\mathbf{x}) \boldsymbol{\Psi}_J^\alpha(\mathbf{x},t) \tag{2}$$

Please cite this article in press as: Belytschko, T., Gracie, R., On XFEM applications to dislocations..., Int. J. Plasticity (2007), doi:10.1016/j.ijplas.2007.03.003

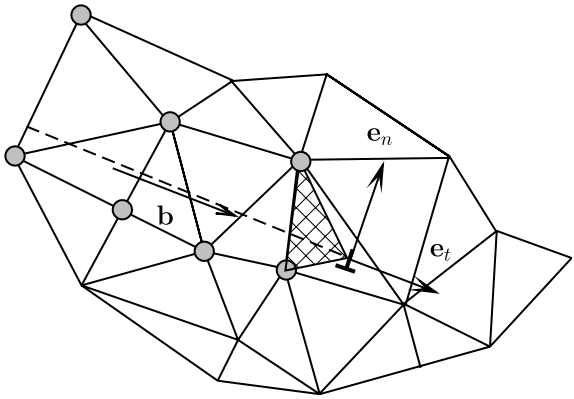

Fig. 1. Illustration of the virtual element, the cross-hatched triangle, which is superimposed on the finite element mesh. The dashed line represents the glide plane. Grey circles represent nodes in the set $\mathscr{S}^\alpha$.

where N_I and $\widetilde{N}_J$ are standard finite element shape functions and $\boldsymbol{u}_I$ are the nodal displacements. For elements cut by the discontinuities $\widetilde{N}_I = N_I$, except in the element containing the core where $\widetilde{N}_I$ are the shape functions of the superimposed element.

The function $\boldsymbol{\Psi}_I^\alpha(\mathbf{x}, t)$ is called the enrichment and introduces the interior discontinuities into the displacement field. We will consider two forms of the enrichment:

1. regularized and compatible

$$\boldsymbol{\Psi}_I^\alpha(\mathbf{x}, t) = (H(f^\alpha(\mathbf{x}, t)) - H(f^\alpha(\mathbf{x}_I, t)))H(g^\alpha(\mathbf{x}, t)) \tag{3}$$

2. incompatible

$$\boldsymbol{\Psi}_I^\alpha(\mathbf{x}, t) = (H(f^\alpha(\mathbf{x}, t)) - H(f^\alpha(\mathbf{x}_I, t)) + H(f^\alpha(\mathbf{x}_I, t))\delta_{IC^\alpha})H(g^\alpha(\mathbf{x}, t)) \tag{4}$$

where $H(\bullet)$ is the Heaviside function given by

$$H(z) = \begin{cases} 0, & z < 0 \\ 1, & z \geqslant 0 \end{cases}. \tag{5}$$

and δ_{IJ} is the Kronecker delta. The first enrichment was previously proposed in Gracie et al. (2007); the second enrichment is a new representation. As indicated by the names, the first enrichment is a regularization of the classical Volterra dislocation field. The shapes of the enrichment functions along the dislocation line are shown in Fig. 2; the classical dislocation model has the shape shown in Fig. 2a.

Eq. (3) employs a linear regularization of the core, Fig. 2b. The linear regularization is mesh dependent; as the approximation is refined, the linear regularization will converge to the classical solution, shown in Fig. 2a. As a result, the total energy of the approximation diverges as the mesh is refined; however, the Peach–Koehler force acting on a dislocation converges. If the total energy is not of interest, and only the movement of dislocations, which is governed by the Peach–Koehler force, then the core behaviour shown in Figs. 2a and 2b can be used as an approximation to the actual dislocation core. When such approximations are too limiting, more accurate core displacement models such as the Peierls–Nabarro model (Peierls, 1940; Nabarro, 1947), can be introduced through the

Please cite this article in press as: Belytschko, T., Gracie, R., On XFEM applications to dislocations..., Int. J. Plasticity (2007), doi:10.1016/j.ijplas.2007.03.003

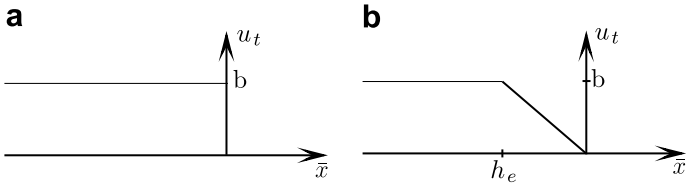

Fig. 2. Illustration of the tangential jump, u_t, along the glide plane from (a) the infinite domain analytical solution for an edge dislocation and the incompatible enrichment (4) and (b) the regularized and compatible enrichment (3).

enrichment of the displacement approximation (2). However, the Peach–Koehler force and the energy outside a core region is almost independent of the regularization.

2.1. Discrete equations

The weak form of the equilibrium equation is the standard principle of virtual work: find $\mathbf{u} \in \mathscr{U}$, such that

$$\int_{\Omega/\Gamma_d} \boldsymbol{\epsilon}(\mathbf{v})^{\mathrm{T}} : \boldsymbol{\sigma}(\boldsymbol{\epsilon}(\mathbf{u}))\mathrm{d}\Omega - \int_{\Omega} \mathbf{g}\cdot\mathbf{v}\mathrm{d}\Omega - \int_{\Gamma_t} \mathbf{t}\cdot\mathbf{v}\,\mathrm{d}\Gamma = 0, \quad \mathbf{v} \in \mathscr{U}_0 \tag{6}$$

where

$$\mathscr{U}_0 = \{\mathbf{u} \in H^1(\Omega/\Gamma_d), \mathbf{u} = 0 \text{ on } \Gamma_u\} \tag{7}$$

$$\mathscr{U} = \{\mathbf{u} \in H^1(\Omega/\Gamma_d), \mathbf{u} = \bar{\mathbf{u}} \text{ on } \Gamma_u\} \tag{8}$$

where $\boldsymbol{\sigma}$ is the Cauchy stress and $\boldsymbol{g}$ is the body force per unit volume. Note that the discontinuities Γ_d are omitted from Ω.

A small strain, linear elastic formulation will be adopted, although the approach can easily be extended to large strain and material nonlinearities. The strain displacement relation is

$$\boldsymbol{\epsilon} = \mathrm{sym}\nabla\mathbf{u} \tag{9}$$

and the constitutive equations is

$$\boldsymbol{\sigma} = \mathbf{C} : \boldsymbol{\epsilon} \tag{10}$$

We place no restriction on $\boldsymbol{C}$; it may be for either an isotropic or an anisotropic material.

Substituting the approximation (2) into the weak form of the equilibrium Eq. (6) the discrete equations to be solved are

$$\mathbf{K}_{uu}\mathbf{d} + \mathbf{K}_{ub}\mathbf{b} = \mathbf{f}^{ext} \tag{11}$$

where $\mathbf{d} = \{\mathbf{u}_1, \mathbf{u}_2, \ldots, \mathbf{u}_{n_n}\}$ are the nodal displacement degrees of freedom of the n_n nodes, and $\mathbf{b}^{\mathrm{T}} = \{\|\mathbf{b}^1\|, \|\mathbf{b}^2\|, \ldots, \|\mathbf{b}^{n_d}\|\}$ is a matrix of Burgers vector magnitudes. The submatrices $\boldsymbol{K}_{uu}$ and $\boldsymbol{K}_{ub}$ and the matrix $\boldsymbol{f}^{\mathrm{ext}}$ are given by

$$\mathbf{K}^{uu}_{IJ} = \int_{\Omega} \mathbf{B}^{\mathrm{T}}_I \mathbf{C}\mathbf{B}_J \,\mathrm{d}\Omega \tag{12}$$

$$\mathbf{K}^{ub}_{I\alpha} = \int_{\Omega} \mathbf{B}^{\mathrm{T}}_I \mathbf{C}\mathbf{D}_\alpha \,\mathrm{d}\Omega \tag{13}$$

Please cite this article in press as: Belytschko, T., Gracie, R., On XFEM applications to dislocations..., Int. J. Plasticity (2007), doi:10.1016/j.ijplas.2007.03.003

$$\mathbf{f}^{ext} = \int_{\Omega} \mathbf{N}^{\mathrm{T}} \mathbf{g}\, \mathrm{d}\Omega + \int_{\Gamma_t} \mathbf{N}^{\mathrm{T}} \mathbf{t}\, \mathrm{d}\Gamma \tag{14}$$

for $I, J \in \mathscr{S}$, and

$$\mathbf{B}_I = \begin{bmatrix} N_{I,x} & 0 \\ 0 & N_{I,y} \\ N_{I,y} & N_{I,x} \end{bmatrix} \tag{15}$$

and

$$\mathbf{D}_\alpha = \sum_{I \in \mathscr{S}^\alpha} \begin{bmatrix} (\widetilde{N}_I \boldsymbol{\Psi}_I^\alpha)_{,x} (\mathbf{e}_t^\alpha \cdot \mathbf{e}_x) \\ (\widetilde{N}_I \boldsymbol{\Psi}_I^\alpha)_{,y} (\mathbf{e}_t^\alpha \cdot \mathbf{e}_y) \\ (\widetilde{N}_I \boldsymbol{\Psi}_I^\alpha)_{,y} (\mathbf{e}_t^\alpha \cdot \mathbf{e}_x) + (\widetilde{N}_I \boldsymbol{\Psi}_I^\alpha)_{,x} (\mathbf{e}_t^\alpha \cdot \mathbf{e}_y) \end{bmatrix} \tag{16}$$

where $\mathbf{e}_t^\alpha$ is a unit vector parallel to the Burgers vector $\boldsymbol{b}^\alpha$ and $\alpha = 1$ to n_D. Note that (12) is the standard stiffness matrix.

In a dislocation dynamics problem, the Burgers vectors are given at every step of the simulation and the displacement can be obtained by solving (11) which gives

$$\mathbf{d} = \mathbf{K}_{uu}^{-1} (\mathbf{f}^{\mathrm{ext}} - \mathbf{K}_{ub} \mathbf{b}) \tag{17}$$

Note that the dislocations are represented in (17) by nodal forces, $\mathbf{K}_{ub}\mathbf{b}$, and that the stiffness matrix, $\boldsymbol{K}_{uu}$, is independent of the geometry and number of dislocations. Furthermore, the stiffness matrix will be identical for the two core models, (3) and (4), whereas the nodal forces, $\mathbf{K}_{ub}\mathbf{b}$, will differ. It can be seen from (17) that the discrete equations are the standard finite element equations and that the effect of the dislocations appears entirely through the external forces, i.e. the right hand side of the equations. Consequently, (a) standard finite element software can easily be adapted to use this method and (b) if a direct solver is used in the DD problems, the stiffness need only be triangulated once and all subsequent steps only involve the far cheaper back-substitution.

2.2. Application of displacement boundary conditions

Boundary conditions are applied in the same manner as in a standard finite element method, i.e. by constraining the nodal degrees of freedom. This can be seen from the displacement approximation (2) and the enrichment functions (3) and (4). At any node on the boundary of the domain, denoted as $\boldsymbol{x}_K$, $\Psi(\mathbf{x}_K) = 0$; therefore, by (2) the nodal displacements at $\boldsymbol{x}_K$ are $\mathbf{u}(\mathbf{x}_K) = \mathbf{u}_K$, as in the standard FEM. Specific displacements along a boundary are imposed by constraining specific $\boldsymbol{u}_K$ in the solution of (11) and (17). For a free boundary no $\boldsymbol{u}_K$ need be constrained, since homogeneous natural boundary conditions follow directly from the weak form. For a fixed boundary which is not intersected by a dislocation glide plane, the constraint $\mathbf{u}_K = 0$ should be imposed. Care should be given when glide planes intersect boundaries where displacement boundary conditions are to be imposed. The displacement along the edge of the boundary elements should be checked to ensure that the desired boundary condition is imposed.

Please cite this article in press as: Belytschko, T., Gracie, R., On XFEM applications to dislocations..., Int. J. Plasticity (2007), doi:10.1016/j.ijplas.2007.03.003

3. Peach–Koehler force

The force $\boldsymbol{F}$ per unit length δs of a dislocation line (Peach and Koehler, 1950), is

$$\mathbf{F} = -\boldsymbol{\xi} \times (\bar{\boldsymbol{\sigma}} \cdot \mathbf{b})\delta s \tag{18}$$

where $\boldsymbol{\xi}$ is a unit vector along the dislocation line s, $\bar{\boldsymbol{\sigma}}$ is the stress at δs from all sources except the self-stress along δs and $\boldsymbol{b}$ is Burgers vector. In superposition methods, the stress $\bar{\boldsymbol{\sigma}}$ on dislocation α in (18) is easily determined as

$$\bar{\boldsymbol{\sigma}}(\mathbf{x}_\alpha) = \sum_{\lambda \neq \alpha}^{n_D} \boldsymbol{\sigma}_\lambda^{\text{self}}(\mathbf{x}_\alpha) + \boldsymbol{\sigma}^{\text{img}}(\mathbf{x}_\alpha) \tag{19}$$

where $\boldsymbol{\sigma}_\lambda^{\text{self}}$ is the self-stress of dislocation λ, $\boldsymbol{\sigma}^{\text{img}}$ is the image stress field and $\boldsymbol{x}_\alpha$ is the location of dislocation core α. This method is not applicable here because the stress at the core as computed by the finite element solution of (11) is not of adequate accuracy. This difference from image field methods such as that of Van der Giessen and Needleman (1995) arises because this method computes the total stress field, which requires more resolution near the core to achieve the same accuracy.

Therefore, we calculate the Peach–Koehler force by a contour integral as proposed by Eshelby (1951). In this method, the Eshelby tensor (also known as the energy–momentum tensor) is integrated over a closed contour about the dislocation core. Eshelby's work was extended by Batra (1987) to nonlinear hyperelastic materials, where the formulation is given in terms of the inverse deformation gradient. For the linear case, as given by Eshelby (1951), the Peach–Koehler force is

$$F_l = -\int_{\Gamma_c} \left[\frac{1}{2}\sigma_{ij}\epsilon_{ij}\delta_{kl} - \sigma_{ik}u_{i,l}\right] n_k \, \mathrm{d}\Gamma \tag{20}$$

where with reference to Fig. 3, Γ_c is any closed contour about the dislocation and $\boldsymbol{n}$ is the unit outward normal of Γ_c. The integral in (20) is widely known as Rice's path-independent J-integral (Rice, 1968).

The stress fields of the finite element models are not continuous. It has been found that the domain form of the J-integral given by Moran and Shih (1987) is more accurate then the contour form (20). The domain form of the J-integral is

$$F_l = -\int_{\Omega_c} \left[\frac{1}{2}\sigma_{ij}u_{i,j}\delta_{kl} - \sigma_{ik}u_{i,l}\right] q_{l,k} \, \mathrm{d}\Omega_c, \text{ no sum on } l \tag{21}$$

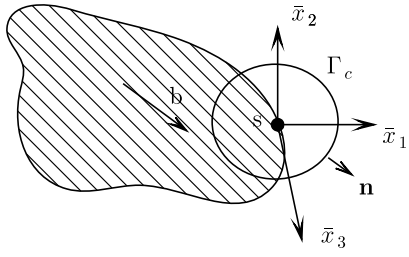

Fig. 3. Conventions for the calculation of the Peach–Koehler force at a point s on a dislocation loop from the J-Integral.

Please cite this article in press as: Belytschko, T., Gracie, R., On XFEM applications to dislocations..., Int. J. Plasticity (2007), doi:10.1016/j.ijplas.2007.03.003

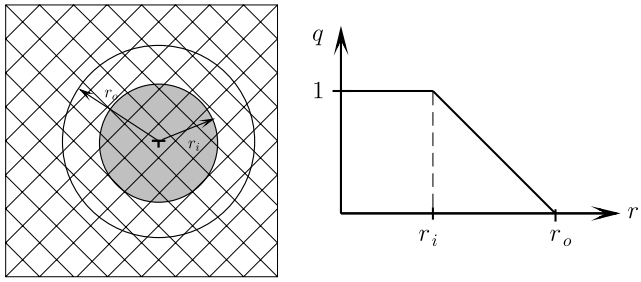

Fig. 4. Left: integration domain definition for the domain form of the J-integral taken about the core of a dislocation. In the shaded circle of radius r_i, the test function $\boldsymbol{q}$ has a value of 1; in the region outside of the circle with radius r_o, the test function $\boldsymbol{q}$ has a value of 0. Right: function $\boldsymbol{q}$ as a function of distance r from the core.

where Ω_c is any domain containing the dislocation core bounded by Γ_c and $\boldsymbol{q}$ is a test function which is continuous with a value of 1 at the dislocation core and zero on Γ_c. For the two-dimensional examples considered below, we defined Ω_c as a disk with an outer radius r_o, centered at the dislocation core. The function $\boldsymbol{q}$ is defined to be 1 at all nodes within a distance r_i from the core and decreases linearly to 0 at r_o. The definition of Ω_c chosen here follows that used by Moës et al. (1999) about crack tips and is illustrated in Fig. 4.

The domain Ω_c must only contain a single dislocation core. So, in order to apply the proposed XFEM method to dislocations, it is desirable that the radius of the integral contour be as small as possible. Selection of Ω_c is discussed in example 4.1. We have found that in general a domain with an outer radius as small as $r_o = 4h_e$ and an inner radius of $r_i = 3h_e$ gives results with an error less than 2%, where h_e is the average element edge length near the dislocation core.

4. Examples

In this section, we consider four examples. The first two examples demonstrate the numerical properties of the method, while the last two examples illustrate the applicability of the proposed method to some problems that may become of interest as DD applications evolve.

In the examples considered, the dislocation core is located at distances of the order of $10^2 b$ from the interfaces. Because only linear elasticity is considered, the accuracy of the method for problems at other distances from the interfaces can be inferred from the results presented. Decreasing the distance of the dislocation from the interface by a given factor and scaling the domain dimensions, element edge lengths and the integration domain of the J-integral by the same factor, yields results with exactly the same relative error.

4.1. Dislocation near a free-surface

To examine the accuracy of this method, we consider an edge dislocation in a semi-infinite domain near a free-surface, as shown in Fig. 5. As discussed by Eshelby (1951), a dislocation near a free-surface can be viewed as a special case of the bimaterial problem where one of the materials has zero stiffness. The free-surface is located at $x = 0$ and the domain is defined by $0 < x < 2L, -L < y < L$. The dislocation is located at a distance

Please cite this article in press as: Belytschko, T., Gracie, R., On XFEM applications to dislocations..., Int. J. Plasticity (2007), doi:10.1016/j.ijplas.2007.03.003

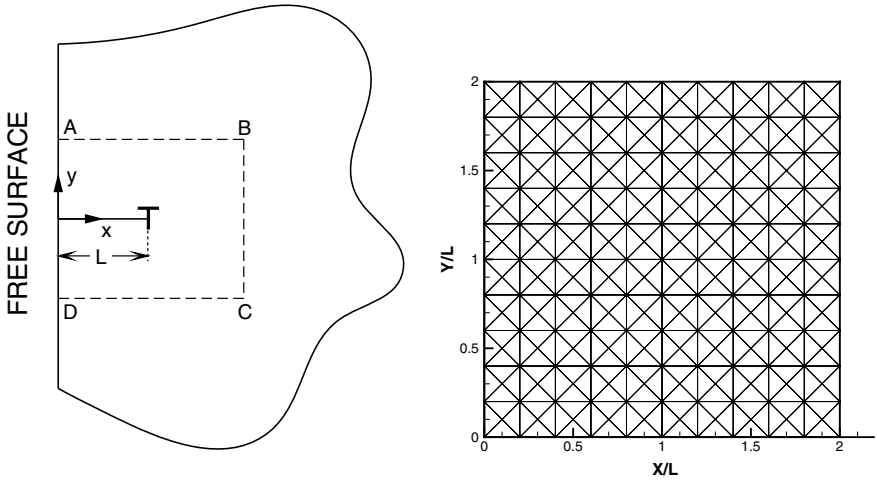

Fig. 5. Left, an edge dislocation in a semi-infinite domain, near a free-surface. Subdomain ABCD is the numerical simulation domain. Right, the structured mesh used to discretize ABCD.

of $L = 500$ nm from the free-surface and the glide plane is perpendicular to the free-surface, along $y = 0$. The elastic constants are $E = 1214.1$ GPa and $\nu = 0.34$ and Burgers vector is $b = 0.21550$ nm. The analytical solution to this problem as given by Head (1953) (after a small typographical correction) is

$$\sigma_x = D\left\{-\frac{y\{3(x-L)^2+y^2\}}{((x-L)^2+y^2)^2}+\frac{y\{3(x+L)^2+y^2\}}{((x+L)^2+y^2)^2}+4Lxy\frac{\{3(x+L)^2-y^2\}}{((x+L)^2+y^2)^3}\right\}$$
$$\sigma_y = D\left\{\frac{y\{(x-L)^2-y^2\}}{((x-L)^2+y^2)^2}-\frac{y\{(x+L)^2-y^2\}}{((x+L)^2+y^2)^2}+4Ly\frac{\{(2L-x)(x+L)^2+(3x+3L)y^2\}}{((x+L)^2+y^2)^3}\right\}$$
$$\sigma_{xy} = D\left\{\frac{(x-L)\{(x-L)^2-y^2\}}{((x-L)^2+y^2)^2}-\frac{(x+L)\{(x+L)^2-y^2\}}{((x+L)^2+y^2)^2}+2L\frac{(L-x)(x+L)^3+6x(x+L)y^3-y^4}{((x+L)^2+y^2)^3}\right\} \tag{22}$$

where $D = Eb/4\pi(1-\nu^2)$. We solve the problem on a subdomain ABCD, as in Fig. 5. Traction boundary conditions corresponding to the analytical solution (22) are applied on the boundaries. A structured mesh of three-node triangles as shown in Fig. 5 is used. In Gracie et al. (2007) we solved this problem and showed that the proposed method approximates the stress fields well and that the strain energy outside of a fixed area around the core converges to the exact solution at the optimal rate of h_e^2 for linear finite elements, where h_e is the element size.

Here, we study the accuracy of the Peach–Koehler force calculated by the domain form of the J-integral, (21). In this study we fix the domain of integration, Ω_c. We have used a ring shaped domain about the dislocation core, as described above, with $r_i/L = 0.1$ and $r_o/L = 0.2$. Fig. 6 shows the convergence of the relative error in the Peach–Koehler force in the glide direction with decreasing element size for both enrichments. In both instances the relative error converges at a rate of about 2.0 with respect to element size. As can be seen from Fig. 6, the new incompatible enrichment yields more accurate Peach–Koehler

Please cite this article in press as: Belytschko, T., Gracie, R., On XFEM applications to dislocations..., Int. J. Plasticity (2007), doi:10.1016/j.ijplas.2007.03.003

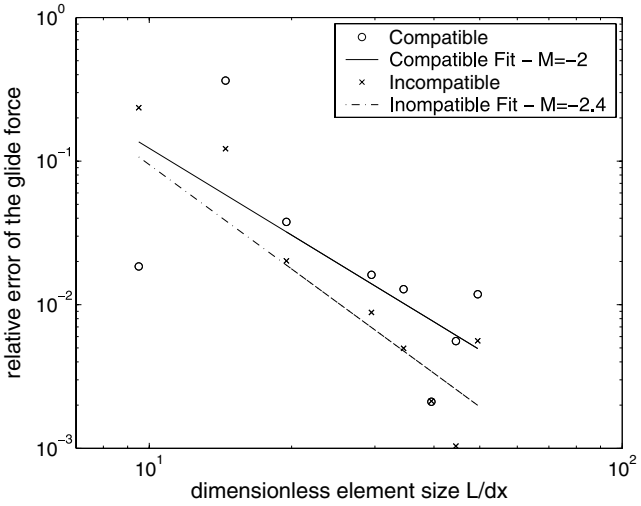

Fig. 6. Convergence of the Peach–Koehler force calculated using the domain form of the J-integral with mesh refinement for an edge dislocation near a free-surface.

forces. However, the values of the Peach–Koehler force are generally comparable, except for certain mesh sizes. Some of these differences are due to the change in accuracy that depends on the relative location of the core in the element. It should be noted that the domain over which the J-integral was computed was larger than would be practical in DD. Such a large domain was used only so that coarse meshes could be included in the convergence study.

We also considered domain integrals of different domain sizes, for a mesh with 60 elements along each boundary, which gives an element size of $h_e = \frac{1}{30}L$. The Peach–Koehler force scaled by L is dependent only on material properties, i.e. $F^{PK} \cdot L = b^2\mu/(4\pi(\nu - 1))$. For the material properties considered here $F^{PK} \cdot L \simeq 3.555$.

For the incompatible enrichment the Peach–Koehler force and the relative error are given in Table 1 in terms of the integration domain size. The first and second rows of Table 1 show that using very small r_i gives very poor results. Comparison of the third to fifth rows shows that when r_i is relatively small, increasing r_i can improve the accuracy of

Table 1
Peach–Koehler force by the domain form of the J-integral for various integration domains for a mesh of 60×60 elements; $h_e \sim \frac{1}{31}L$ is the element size

r_i	r_o	$F_{PK} \cdot L$	Relative error in F_{PK}
$1h_e$	$3h_e$	−1.995	0.44
$1.5h_e$	$3h_e$	−4.307	0.21
$1.5h_e$	$6h_e$	−3.784	6.4×10^{-2}
$2h_e$	$6h_e$	−3.459	2.7×10^{-2}
$3h_e$	$6h_e$	−3.522	9.1×10^{-3}
$3h_e$	$10h_e$	−3.499	1.6×10^{-2}
$6h_e$	$10h_e$	−3.482	2.0×10^{-2}
$6h_e$	$12h_e$	−3.481	2.1×10^{-2}

Please cite this article in press as: Belytschko, T., Gracie, R., On XFEM applications to dislocations..., Int. J. Plasticity (2007), doi:10.1016/j.ijplas.2007.03.003

the J-integral. In both cases this is a reflection of the fact that the stress field at the core is less accurate than that away from the core. The last three rows show that for very large domains, increasing r_i decreases the accuracy slightly. Therefore, the inner radius of the integration domain should be chosen sufficiently far from the core, but still in the vicinity of the core.

4.2. Dislocation near a bimaterial interface

Next we consider an edge dislocation near a bimaterial interface between two semi-infinite domains, as shown in Fig. 7. Bimaterial problems are a particular target of this method since they are difficult to treat by superposition methods.

The bimaterial interface is located along the plane $x = L/2$. An edge dislocation with Burgers vector $b = 0.2551$ nm and with a glide plane along the plane $y = L/2$ is considered. The core is located at $x = L/2 + h$. In the subdomain $x > L/2$ the elastic modulus $E_1 = 121.41$ GPa and Poisson's ratio $\nu_1 = 0.34$; in the subdomain $x < L/2$, $E_2 = 0.1E_1$ and $\nu_2 = 0.3$.

The solution to this problem was given by Head (1953), and later used to study the Peach–Koehler force on a dislocation near a bimetallic interface by Dundurs and Sendeckyj (1965). Further clarification of the solution was provided by Lubarda (1997) in the context of dislocation arrays near bimaterial interfaces. The ratio of shear moduli is given by $\Theta = \mu_2/\mu_1$ and for plane strain $\kappa_i = 3 - 4\nu_i$. The glide force acting on a dislocation at a distance h from a bimaterial interface as given by Dundurs and Sendeckyj (1965) is

$$F_g = \frac{-(\mathscr{B} + \mathscr{A})\mu_1 b^2}{2\pi(\kappa_1 + 1)h} \tag{23}$$

where $\mathscr{A}$ and $\mathscr{B}$ are given by

$$\mathscr{A} = \frac{1 - \Theta}{1 + \Theta\kappa_1}, \quad \mathscr{B} = \frac{\kappa_2 - \Theta\kappa_1}{\kappa_2 + \Theta} \tag{24}$$

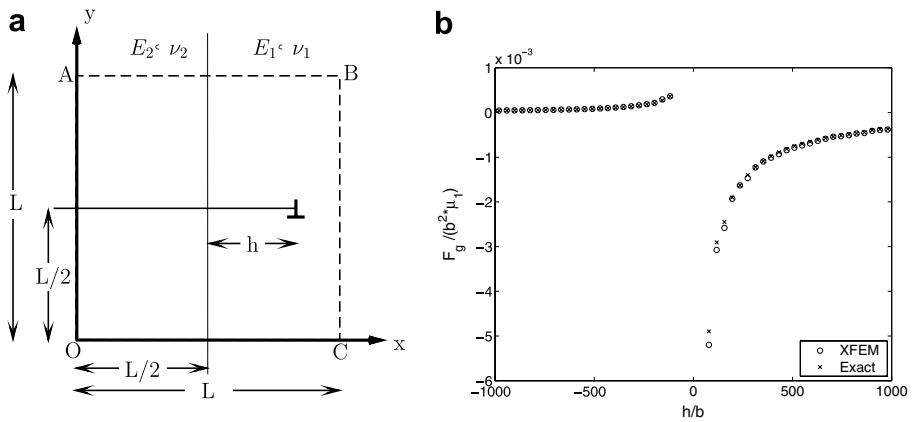

Fig. 7. (a) Nomenclature for an edge dislocation near a bimaterial interface between two semi-infinite domains. (b) comparison of the glide component of the Peach–Koehler force obtained by the proposed method with the exact result.

Please cite this article in press as: Belytschko, T., Gracie, R., On XFEM applications to dislocations..., Int. J. Plasticity (2007), doi:10.1016/j.ijplas.2007.03.003

We consider a square $L \times L$ domain ABCD, $L = 1$ μm, as shown in Fig. 7. Along the edges of the domain, traction boundary conditions corresponding to the exact solution are applied; the expressions for the stress fields are given in Lubarda (1997). We discretize the domain with an unstructured mesh of 13,320 three-node triangular elements giving an average element edge length of about $15b$.

In Fig. 7b, the glide component of the Peach–Koehler force obtained by the proposed method is compared to that from (23) for various distances, h, from the material interface. As can be seen, the glide force for the incompatible enrichment calculated with the domain form of the J-integral with $r_i = 3h_e$ and $r_o = 5h_e$ compares well with the exact result. As the dislocation approaches the interface, the accuracy decreases somewhat as a result of insufficient mesh resolution. When the number of elements separating the dislocation core from the interface was less than 5, we used $r_o = h$ and $r_i = h/2$ for the domain integral, yielding less accurate results. Mesh refinement near the interface can be used to increase the accuracy of the glide force calculation. Such refinement is easily accomplished since the element edges do not have to conform to the glide plane.

The convergence of the glide component of the Peach–Koehler force for both the compatible and incompatible enrichments is shown in Fig. 8, for $h/L = 0.2$. In this example, the incompatible enrichment is again more accurate than the compatible and regularized enrichment for fine meshes. For both enrichments the relative error decreases non-monotonically with element size at a rate slightly greater than 1. The non-monotonic nature of the convergence curve is most likely a result of the fact that the size of the superimposed element depends on not only the underlying mesh size but also the location of the dislocation core in the underlying element.

Contour plots of the shear stress, σ_{xy}, and for the normal stress, σ_{yy}, for the regularized and compatible enrichment are shown in Figs. 9 and 10, respectively, with the corresponding contours for the exact solution for $h/L = 0.2$. The stress contours show good agreement with the exact solution fields. We see that σ_{yy} is discontinuous across the material

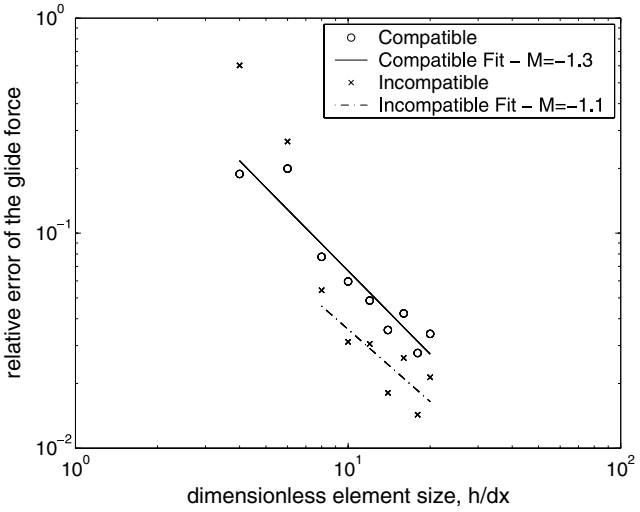

Fig. 8. Convergence of the glide force on an edge dislocation near a bimaterial interface.

Please cite this article in press as: Belytschko, T., Gracie, R., On XFEM applications to dislocations..., Int. J. Plasticity (2007), doi:10.1016/j.ijplas.2007.03.003

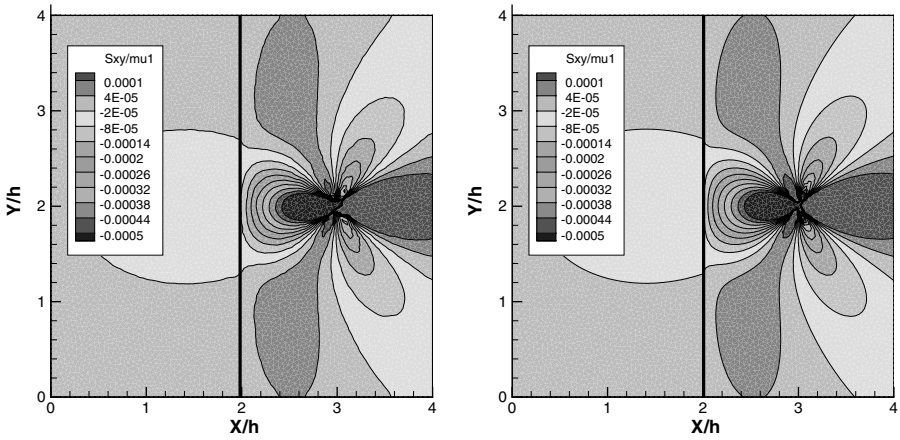

Fig. 9. Comparison of the shear stress, σ_{xy}, contours from the proposed method (right) with those of the exact solution (left) for an edge dislocation near a bimaterial interface.

interface, but that σ_{xy} is continuous, as expected. Furthermore, mesh refinement near the dislocation core would improve the accuracy of the stresses in the vicinity of the core.

4.3. Slip-plane misorientation

We consider an edge dislocation in a square $W \times W$, $W = 1$ μm, bimaterial plate, as shown in Fig. 11; the body is supported only sufficiently to preclude rigid body motion, so the edges are otherwise free. The body is divided along the plane $x = W/2$. In the domain $x > W/2$ the elastic constants are $E_1 = 121.41$ GPa and $\nu_1 = 0.34$, while in the domain $x < W/2$, $E_2 = 0.1E_1$ and $\nu_2 = 0.3$. An edge dislocation is located in the domain $x > W/2$ at a distance of h from the point $(W/2, W/2)$ and oriented at an angle of θ from the x-axis. The slip plane of the dislocation extends from the dislocation core to the point $(W/2, W/2)$, where the glide plane crosses the material interface. Due to slip-plane misorientation, the slip plane continues in the domain $x < W/2$ along the plane $y = W/2$. The magnitude of the Burgers vector, $b = 0.8551$ nm, is assumed to be the same along both the horizontal and inclined portions of the glide plane. Different Burger's vector magnitudes could have been adopted for each material.

This problem is solved using an unstructured mesh of 13,320 three node triangular elements with an average element edge length of about $15b$. For $h/W = 0.25$ and $\theta = \pi/6$ the shear stress contours are shown in Fig. 12. From these contours we can see that the proposed method predicts a residual dislocation at the material interface. The residual dislocation results from the incompatibility of the displacements where the slip plane intersects the material interface.

The glide and climb forces acting on an edge dislocation with $h/W = 0.1$ for various values of θ between $-\frac{\pi}{6}$ and $\frac{\pi}{6}$ are shown in Fig. 13. The climb force is antisymmetric with respect to θ, while the glide force is symmetric, as expected. Because an unstructured mesh was used and because the method exhibits some mesh dependence, small perturbations from perfect symmetry and antisymmetry are observed. The maximum glide force occurs when $\theta = 0$; however, glide forces of similar magnitude act to move the dislocation towards the material interface when $\theta = \pm\frac{\pi}{6}$.

Please cite this article in press as: Belytschko, T., Gracie, R., On XFEM applications to dislocations..., Int. J. Plasticity (2007), doi:10.1016/j.ijplas.2007.03.003

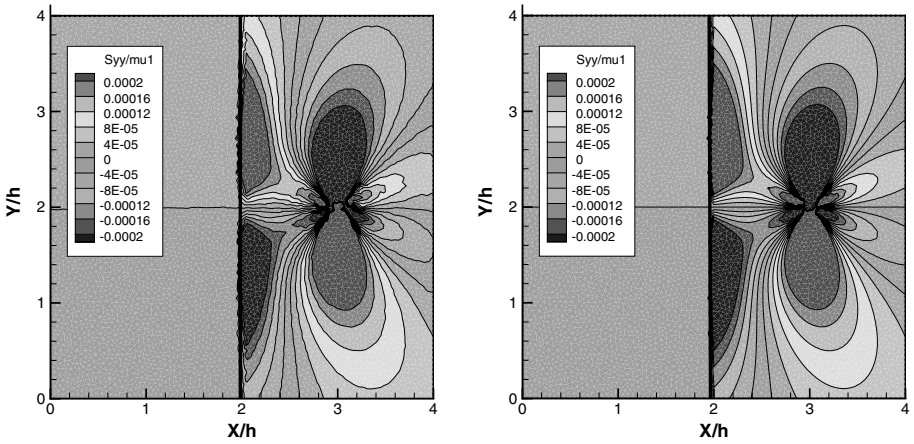

Fig. 10. Comparison of the y-direction stress, σ_{yy}, contours from the proposed method (right) with those of the exact solution (left) for an edge dislocation near a bimaterial interface.

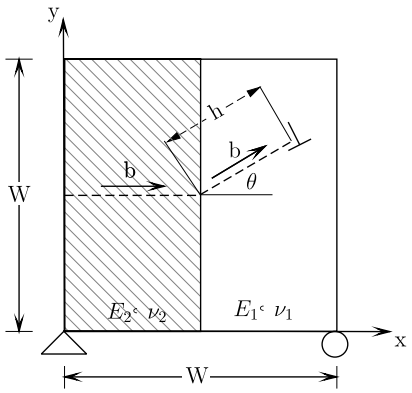

Fig. 11. Edge dislocation in a simply supported bimaterial body with slip plane misorientation across the material interface. Dashed line represents the material interface; dotted line represents the slip plane.

4.4. Finite body with multiple material interfaces

To illustrate the capability of the method to deal with more complicated geometries, we consider a multimaterial body with four different materials and five material interfaces, as shown in Fig. 14. The domain dimensions are $h \times L$ where $h = 1000$ nm $= 1169.5b$ and $L = 2h$. The elastic properties in each section of the body are $E_1 = 1000$ GPa, $v_1 = 0.34$, $E_2 = 0.1E_1$, $v_2 = 0.30$, $E_3 = 2 \cdot E_1$, $v_3 = 0.2$, and $E_4 = 0.005E_1$, $v_{14} = 0.25$. The bottom edge of the body is rigidly constrained while the top edge is prescribed a displacement corresponding to 2% shear strain. Ten slip planes parallel to the x-axis are evenly distributed throughout the system. Along each slip plane n dislocations are randomly distributed. Each dislocation is assumed to have the same Burgers vector $b = 0.8551$ nm directed in the x-direction. This problem would be challenging for superposition methods since the

Please cite this article in press as: Belytschko, T., Gracie, R., On XFEM applications to dislocations..., Int. J. Plasticity (2007), doi:10.1016/j.ijplas.2007.03.003

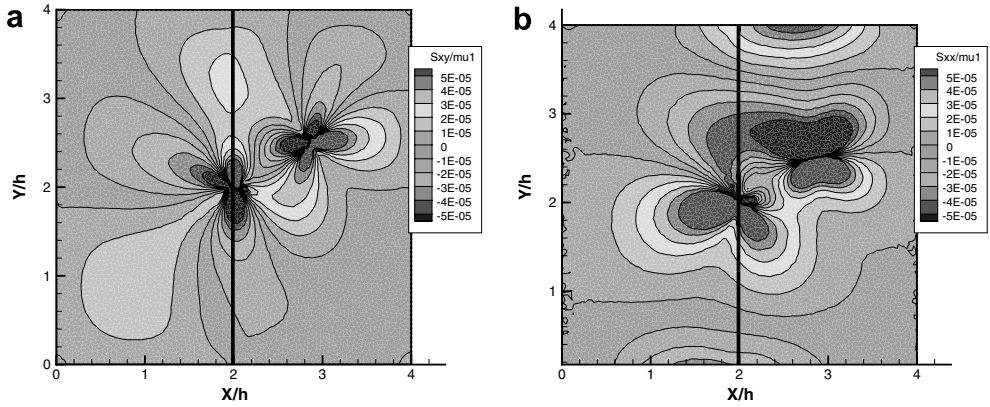

Fig. 12. Contours of: (a) the shear stress σ_{xy} and (b) the x-direction stress σ_{xx} for an edge dislocation in a bimaterial plate with slip plane misorientation across the material interface. h is the distance of the core of the dislocation in the bulk from that at the material interface.

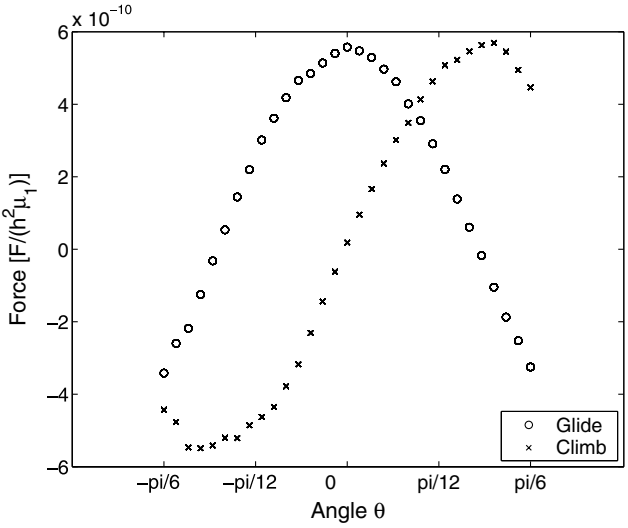

Fig. 13. Glide and climb force acting on the edge dislocation from Fig. 11 for various values of θ and $h/W = 0.1$.

body has several materials, finite dimensions, and the material interfaces are not parallel. The relative reduction in the force required to produce a 2% shear strain is shown in Fig. 15. The required force decreases linearly with an increase in the number of dislocations because the number of slip planes containing dislocations was fixed. If the number of these slip planes was varied, the required force would not decrease linearly with an increase in the number of dislocations. A more realistic analysis of the above system would require a full DD simulation, likely in 3D. However, the potential of this method to solve problems involving the interaction of dislocations with material interfaces has been demonstrated.

Please cite this article in press as: Belytschko, T., Gracie, R., On XFEM applications to dislocations..., Int. J. Plasticity (2007), doi:10.1016/j.ijplas.2007.03.003

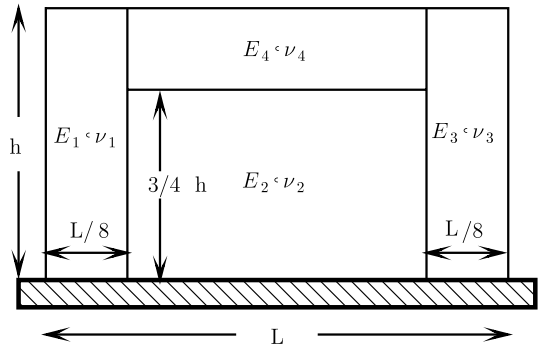

Fig. 14. Nomenclature for the problem of a body with multiple materials.

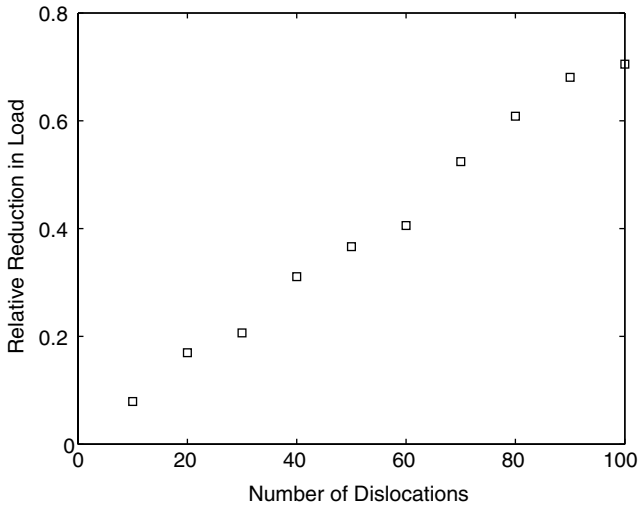

Fig. 15. Percent reduction in applied force required to produce a 2% shear strain in the multimaterial problem.

5. Conclusions

An extended finite element method (XFEM) for modelling dislocations in systems with multiple arbitrary material interfaces was presented. The method uses a standard finite element method (FEM) to determine the total stress field subject to prescribed internal discontinuities, i.e. the dislocation slip.

Since the method presented here uses a FEM to determine the *total* stress field, the mesh must be sufficiently refined to capture the high gradients of the stress field near the core. So more resolution is needed than in the method of Van der Giessen and Needleman (1995) where only the image stress field is determined by the FEM. The method has two advantages over superposition and image field methods. (a) The method scales linearly with the number of dislocations for a given mesh since the Peach–Koehler force can be determined from local quantities and its computational complexity does not depend on the number of

Please cite this article in press as: Belytschko, T., Gracie, R., On XFEM applications to dislocations..., Int. J. Plasticity (2007), doi:10.1016/j.ijplas.2007.03.003

dislocations in the domain. (b) The method is applicable to problems of multiple arbitrary material interfaces and is easily extended to anisotropic materials.

At this time it is not clear if the proposed method offers an advantage over superposition based models for DD in a single isotropic material. However, the goal of the work here is not to replace superposition models in their current applications, but to present a method capable of treating new applications involving material interfaces, which are difficult for existing methods.

We have examined the suitability and accuracy of contour integral methods to calculate the Peach–Koehler force. We have shown that accuracies of about 98% can be obtained even with contours of moderate dimensions (between 3 and 5 times the element size in the calculations reported). This would be disadvantageous for dislocation dynamics simulations, since the dislocations are often in close proximity in such simulations. However, the contour integral method for the Peach–Koehler force can be advantageous since it requires only local quantities and so does not directly depend on the number of dislocations in the domain.

Compatible and incompatible enrichments have been considered. The incompatible enrichment yields more accurate results; however, the accuracy of the two enrichments is of the same order, which suggests that for the cases considered here the details of the core representation do not significantly affect the results.

To demonstrate the accuracy and convergence of the method for problems with interfaces, we have reported calculations for a single edge dislocation adjacent to an interface and for an edge dislocation interacting with a bimaterial interface. In both problems, comparison to analytical results were made. For the discretizations considered, relative errors of 2% were obtained for element sizes of 0.1–0.075 times the separation distance of the dislocation from the interface. The linear elements we have programmed so far have a limited ability to approximate the high strain gradients in the vicinity of the dislocation core. The use of higher-order elements is expected to greatly improve the accuracy of the method.

It is unclear at this time exactly what the niche for this method will be. None of the available methods have the versatility of the proposed method in terms of geometry, material properties and nonlinearities. The method requires more resolution than methods based on Green's functions and image fields, but the required resolution is comparable to the Phase Field Method which has solved very large problems, see Wang et al. (2001). Furthermore, its compatibility with standard FEM software should prove attractive.

Acknowledgements

This work was supported by the Army Research Office under Grant W911NF-05-0049, the National Science Foundation under Grant CMS00304472 and the Natural Sciences and Engineering Research Council of Canada under a graduate scholarship.

References

Amodeo, R.J., Ghoniem, N.M., 1990. Dislocation dynamics. I. A proposed methodology for deformation micromechanics. Phys. Rev. B 41, 6958–6967.

Balint, D.S., Deshpande, V.S., Needleman, A., Van der Giessen, E., 2006. Size effects in uniaxial deformation of single and polycrystals: a discrete dislocation plasticity analysis. Modell. Simulat. Mat. Sci. Eng. 14 (3), 409–422.

Please cite this article in press as: Belytschko, T., Gracie, R., On XFEM applications to dislocations..., Int. J. Plasticity (2007), doi:10.1016/j.ijplas.2007.03.003

Batra, R.C., 1987. The force on a lattice defect in an elastic body. J. Elasticity 17 (1), 3–8.
Belytschko, T., Black, T., 1999. Elastic crack growth in finite elements with minimal remeshing. Int. J. Num. Meth. Eng. 45, 601–620.
Belytschko, T., Moës, N., Usui, S., Parimi, C., 2001. Arbitrary discontinuities in finite elements. Int. J. Num. Meth. Eng. 50, 993–1013.
Canova, G., Brechet, Y., Kubin, L.P., DeVincre, B., Pontikis, V., Condat, M., 1993. 3d simulation of dislocation motion on a lattice: application to the yield surface of single crystals. Solid State Phenom., 101–106.
Dundurs, J., Sendeckyj, G.P., 1965. Behavior of an edge dislocation near a bimetallic interface. J. Appl. Phys. 36 (10), 3353–3354.
Eshelby, J.D., 1951. The force on an elastic singularity. Philos. Trans. Roy. Soc. Lond. Ser. A, Math. Phys. Sci. 244 (877), 87–112.
Espinosa, H.D., Panico, M., Berbenni, S., Schwarz, K.W., 2006. Discrete dislocation dynamics simulations to interpret plasticity size and surface effects in freestanding fcc thin films. Int. J. Plasticity 22 (11), 2091–2117.
Fivel, M.C., Gosling, T.J., Canova, G.R., 1996. Implementing image stresses in a 3d dislocation simulation. Modell. Simulat. Mat. Sci. Eng. 4 (6), 581–596.
Ghoniem, N.M., Han, X., 2005. Dislocation motion in anisotropic multilayer materials. Philos. Mag. 85 (24), 2809–2830.
Ghoniem, N.M., Tong, S.-H., Sun, L.Z., 2000. Parametric dislocation dynamics: a thermodynamics-based approach to investigations of mesoscopic plastic deformation. Phys. Rev. B 61 (2), 913–927.
Gracie, R., Ventura, G., Belytschko, T., 2007. A new fast method for dislocations based on interior discontinuities. Int. J. Num. Meth. Eng. 69, 423–441.
Han, X., Ghoniem, N.M., 2005. Stress field and interaction forces of dislocations in anisotropic multilayer thin films. Philos. Mag. 85 (11), 1205–1225.
Head, A.K., 1953. Edge dislocations in inhomogeneous media. Proc. Phys. Soc. Sec. B 66 (9), 793–801.
Lemarchand, C., Devincre, B., Kubin, L.P., 2001. Homogenization method for a discrete-continuum simulation of dislocation dynamics. J. Mech. Phys. Solids 49 (9), 1969–1982.
Lubarda, V.A., 1997. Energy analysis of dislocation arrays near bimaterial interfaces. Int. J. Solids Struct. 34 (9), 1053–1073.
Moës, N., Dolbow, J., Belytschko, T., 1999. A finite element method for crack growth without remeshing. Int. J. Num. Meth. Eng. 46, 131–150.
Moran, B., Shih, C.F., 1987. A general treatment of crack tip contour integrals. Int. J. Fract. 35 (4), 295–310.
Nabarro, F.R.N., 1947. Dislocations in a simple cubic lattice. Proc. Phys. Soc. 59 (2), 256–272.
Nicola, L., Van der Giessen, E., Needleman, A., 2005. Size effects in polycrystalline thin films analyzed by discrete dislocation plasticity. Thin Solid Films 479 (1-2), 329–338.
Peach, M., Koehler, J.S., 1950. The forces exerted on dislocations and the stress fields produced by them. Phys. Rev. 80 (3), 436–439.
Peierls, R., 1940. The size of a dislocation. Proc. Phys. Soc. 52 (1), 34–37.
Polonsky, I.A., Keer, L.M., 1996. Simulation of microscopic elastic–plastic contacts by using discrete dislocations. Proc. Math. Phys. Eng. Sci. 452 (1953), 2173–2194.
Rice, J.R., 1968. A path independent integral and approximate analysis of strain concentration by notches and cracks. J. Appl. Mech. 35 (2), 379–386.
Shehadeh, M.A., Zbib, H.M., de la Rubia, T.D., 2005. Multiscale dislocation dynamics simulations of shock compression in copper single crystal. Int. J. Plasticity 21 (12), 2369–2390.
Van der Giessen, E., Needleman, A., 1995. Discrete dislocation plasticity: a simple planar model. Modell. Simulat. Mat. Sci. Eng. 3, 689–735.
Ventura, G., Moran, B., Belytschko, T., 2005. Dislocations by partition of unity. Int. J. Numer. Meth. Eng. 62 (11), 1463–1487.
Volterra, V., 1907. Sur l'équilibre des corps élastiques multiplement connexes. Ann. Sci. 'École Norm. Supérieure Sér. 3 (24), 401–517.
Wang, Y.U., Jin, Y.M., Cuitino, A.M., Khachaturyan, A.G., 2001. Nanoscale phase field microelasticity theory of dislocations: model and 3D simulations. Acta Mater. 49 (10), 1847–1857.
Xiang, Y., Cheng, L.T., Srolovitz, D.J., Weinan, E., 2003. A level set method for dislocation dynamics. Acta Mater. 51 (18), 5499–5518.
Zbib, H.M., Rhee, M., Hirth, J.P., 1998. On plastic deformation and the dynamics of 3d dislocations. Int. J. Mech. Sci. 40, 113–127.

Please cite this article in press as: Belytschko, T., Gracie, R., On XFEM applications to dislocations..., Int. J. Plasticity (2007), doi:10.1016/j.ijplas.2007.03.003